THESIS FOR THE DEGREE OF DOCTOR OF PHILOSOPHY

IN THERMO AND FLUID DYNAMICS

Prediction of Cooling Air Flow in Electric Generators

by

Pirooz Moradnia

Department of Applied Mechanics
CHALMERS UNIVERSITY OF TECHNOLOGY
Göteborg, Sweden, 2013

Prediction of
Cooling Air Flow
in Electric Generators
Pirooz Moradnia
ISBN 987-91-7385-842-7

Doktorsavhandling vid Chalmers tekniska högskola
Ny serie nr. 3523
ISSN 0346-718X

Division of Fluid Dynamics
Department of Applied Mechanics
Chalmers University of Technology
SE-412 96 Göteborg, Sweden

Telephone +46-(0)31-7721000
Fax +46-(0)31-180976

Cover: CAD model of the electric generator used in this work.

Printed at Chalmers Reproservice
Göteborg, Sweden, 2013

Prediction of
Cooling Air Flow
in Electric Generators

PIROOZ MORADNIA

Department of Applied Mechanics
Chalmers University of Technology

Abstract

The cooling air flow in hydro power electric generators is investigated experimentally and numerically. A fully predictive numerical approach is presented and validated, in which the inlet and outlet boundaries are eliminated from the computational domain. Instead, a part of the space outside the machine is included in the computational domain, allowing for recirculation of the cooling air. The predicted flow is therefore driven solely by the rotation of the rotating parts of the generator. In this way, the predicted flow field is independent of any experimental data at the inlet, and is determined completely by the solution.

Using the fully predictive approach, a number of parametric numerical studies are performed on the rotor and stator geometries. The effect of adding geometrical details to the rotor and stator are investigated, and stator baffles and rotor fan blades are concluded to increase the volume flow rate through the machine. The volume flow rate through the machine is found to vary linearly with the rotor rotational speed, while the required rotor axial power increases cubically with the rotor rotational speed.

The numerical results are validated against experimental measurements in a real electric generator. Flow visualizations, and 5-hole probe and total pressure measurements are performed. A comparison of the numerical results and the experimental data reveals a good qualitative prediction of the flow by the fully predictive numerical approach. The sensitivity of the numerical results to different choices of inlet boundary conditions is also investigated. The level of detail in the boundary conditions proves to play an important role in predicting correct flow features.

A half-scale laboratory model, based on the above studied electric generator, is specifically designed and manufactured for experimental studies of the cooling air flow. The measurement accuracy in the half-scale model is significantly improved compared to that in the real generator. The model is provided with static pressure holes and optical

access for flow measurements using Particle Image Velocimetry (PIV). The fully predictive numerical approach is shown to yield quantitatively similar results as the experimental flow measurements. The numerical simulations are also performed with inlet and outlet boundary conditions, by specifying the inlet volume flow rates from the experimental measurements. The results of the fully predictive numerical approach are shown to agree better with the experimental data, than those of the simulations with inlet and outlet boundary conditions.

Keywords: CFD, Electric Generator, Multiple Reference Frame, Flow Prediction, OpenFOAM, Experimental Measurements, PIV, Total Pressure Measurements, 5-hole Pressure Probe Measurements

List of Publications

This thesis is based on the work contained in the following five papers.

I P. Moradnia and H. Nilsson, 2011, "A Parametric Study of the Air Flow in an Electric Generator Through Stepwise Geometry Modifications", *ECCOMAS 2011*, An ECCOMAS Thematic Conference, CFD and OPTIMIZATION, (040) ISBN/ISSN: 978-605-61427-4-1, Antalya, Turkey.

Division of work Moradnia produced all the numerical results and wrote the paper. Nilsson supervised the planning, analysis and writing. The final paper was proofread by both authors.

II P. Moradnia, V. Chernoray and H. Nilsson, 2011, "Experimental and Numerical Investigation of the Cooling Air Flow in an Electric Generator", *HEFAT 2011*, 8th International Conference on Heat Transfer, Fluid Mechanics and Thermodynamics, pp. 242-249, Mauritius.

Division of work Moradnia produced all the numerical results, was actively involved in preparing the experimental rig for the measurements, performed the flow visualizations and measurements, analyzed the results, and wrote the paper. Chernoray was involved in setting up the flow visualizations and measurements, and processed the experimental data. Nilsson supervised the planning, experimental preparations, analysis and writing. The final paper was proofread by all authors.

III P. Moradnia, V. Chernoray and H. Nilsson, 2012, "Experimental and Numerical Study of Cooling Air Flow in a Hydroelectric Generator", *ETMM9*, European Research Community On Flow, Turbulence and Combustion, Thesaloniki, Greece.

Division of work Moradnia produced all the numerical results, was actively involved in preparing the experimental rig for the

measurements, performed the flow visualizations and measurements, analyzed the results, and wrote the paper. Chernoray was involved in setting up the flow visualizations and measurements, and processed the experimental data. Nilsson supervised the planning, experimental preparations, analysis and writing. The final paper was proofread by all authors.

IV P. Moradnia, V. Chernoray and H. Nilsson, 2013, "Assessment of a Fully Predictive CFD Approach, Using Experimental Data of Cooling Air Flow in an Electric Generator", submitted for journal publication.

Division of work Moradnia produced all the numerical results, was actively involved in preparing the experimental rig for the measurements, performed the flow visualizations and measurements, analyzed the results, and wrote the paper. Chernoray was involved in setting up the flow visualizations and measurements, and processed the experimental data. Nilsson supervised the planning, experimental preparations, analysis and writing. The final paper was proofread by all authors.

V P. Moradnia, M. Golubev, V. Chernoray and H. Nilsson, 2013, "Cooling Air Flow in an Electric Generator Model – An Experimental and Numerical Study", submitted for journal publication.

Division of work Moradnia produced all the numerical results, was actively involved in the design, manufacturing, and preparations of the experimental rig for the measurements, analyzed the results, and wrote the paper. Golubev performed the flow visualizations and measurements, and processed the experimental data. Chernoray supervised the construction of the experimental model and the experimental measurements. Nilsson supervised the planning, the construction of the experimental model, the analysis and writing. The final paper was proofread by all authors.

Acknowledgments

My special gratitude to Håkan Nilsson for the great supervision and courage during the past five years. I am so proud of having worked with you and appreciate all your support and endeavor.

The technical advice received from Tage Carlsson, Johan Westin, Daniel Rundström and Bo Hernnäs was a great resource which guided the present research and is greatly acknowledged.

The experimental preparations and studies in this work were performed thanks to Valery Chernoray and Maxim Golubev, and with their great effort.

The access to the generator rig at Uppsala University was provided by Urban Lundin and Mattias Wallin, who also put a great deal of time on the design modifications.

Many thanks to our colleagues at the division of fluid dynamics for the nice work environment. I was specially lucky to have Guillaume Jourdain and Bastian Nebenführ as office-mates, without whom the work wouldn't be as enjoyable.

Knowing Martin Svensson was a great chance to practice personal development. Thanks Martin for all viewpoints, and thanks Sofia Månsson for this opportunity.

My three month-stay in Canada was an exceptional experience which became more pleasant thanks to the colleagues at Hydro-Quebec. I am especially grateful to Maryse Page for all the fantastic support, it was a pleasure working with you. I also had the opportunity of meeting Samuel Cupillard, Laurent Tôn-Thât, and Nicolas Laroche, three wonderful gentlemen with whom I lost the track of time!

The endless love and unconditional support I have always received from my family is beyond comparison. Thanks Davood, Minoo, Hoda, Mahtab and Shahrouz for being there all time for me.

The research presented in this thesis was carried out as a part of the "Swedish Hydropower Centre - SVC". SVC has been established by the Swedish Energy Agency, Elforsk and Svenska Kraftnät together with Luleå University of Technology, The Royal Institute of Technology, Chalmers University of Technology and Uppsala University. Participating hydro power companies are: Andritz Hydro, E.ON Vattenkraft

Sverige, Fortum Generation, Holmen Energi, Jämtkraft, Karlstads Energi, Linde Energi, Mälarenergi, Skellefteå Kraft, Sollefteå-forsens, Statkraft Sverige, Statoil Lubricants, Sweco Infrastructure, Sweco Energuide, SveMin, Umeå Energi, Vattenfall Research and Development, Vattenfall Vattenkraft, VG Power and WSP.

The computational facilities are provided by C^3SE, the center for scientific and technical computing at Chalmers University of Technology, and SNIC, the Swedish National Infrastructure for Computing.

Contents

Chapter 1

Introduction

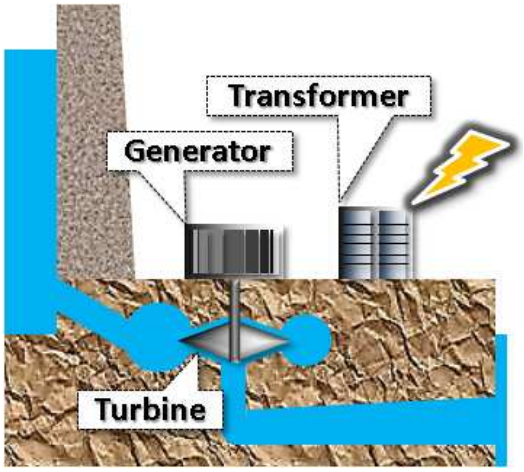

Figure 1.1: A schematic view of a hydro electric power plant

HYDRO power is the most efficient electric power generation method reaching up to 95% efficiency. It plays an important role in the electric power supply in Sweden, producing nearly half of the total electric power in the country. Hydro electric power plants are used to convert the mechanical energy of the flowing water into electricity. Figure 1.1 shows a schematic view of a hydro electric power plant. Collected from a reservoir with high hydrostatic head, the water flow drives a turbine, which in turn drives an electric generator that generates electric power through magnetic induction. A transformer is used to decrease the induced electric current by increasing the voltage, while preserving the power. The electricity is then transmitted to the network, for distribution to the customers.

Like any other complicated system, a hydro electric power plant is comprised of a large number of different components, any of which

should be carefully designed and optimized to yield the highest possible efficiency. The majority of the hydro power plants in Sweden were constructed during the 1950s and 60s, and many of them are in need of refurbishment. Design modifications and improvements to these systems can contribute to a considerably increased total electric power generation. An increased power generation increases the heat, which should be removed from the system.

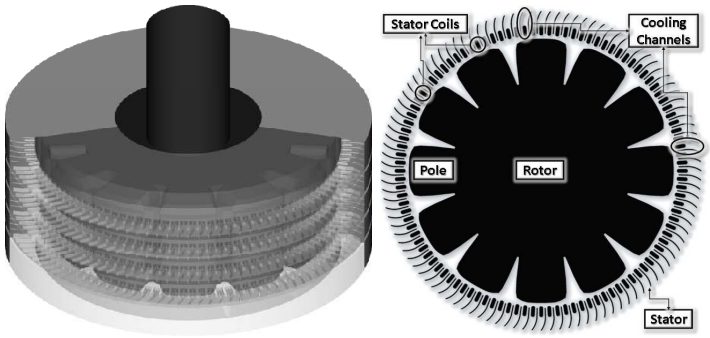

(a) CAD model (b) Cross-section

Figure 1.2: CAD model and cross-section of an electric generator

The focus in the present work is on electric generators, in which the conversion of the mechanical energy into electricity takes place. Figure 1.2 shows a CAD model and a cross-section of an electric generator. An electric generator is made up of a rotor and a stator. The rotor is composed of a number of electromagnetic poles, and is connected to the turbine runner through a shaft. The stator is the stationary part surrounding the rotor, and is comprised of a number of electric coils. An alternating electric current is induced in the electric coils of the stator as a result of the relative movement of the magnetic field of the rotor poles.

1.1 Losses in Electric Generators

The process of conversion of the mechanical energy into electricity in electric generators includes energy losses. The energy losses are divided into three main classes:

1) Electric losses, due to the electric resistance in the stator coils

2) Magnetic losses, mainly due to the eddy currents appearing as a result of the rotating magnetic field of the rotor relative to the stator core

3) Mechanical losses due to cooling air flow and friction in bearings

The losses generate heat, which raises the temperature of the machine components and leads to a change in the material properties. This includes the temperature dependent electric resistance. A working temperature beyond the design range may thus result in a lower efficiency. Further, the life-time of certain components, such as insulation materials, is affected by high (or varying) temperatures. It is therefore important to remove the heat to keep the machines at a stable and even temperature near their best operating points. Electric generators are cooled by means of convection. A large number of cooling channels are provided in the stator body to allow for the passage of cooling air to cool down the stator coils, see Fig. 1.2(b). The rotor acts as a fan which builds up a pressure difference between the inside and the outside of the stator, forcing the air flow through the stator cooling channels.

1.2 Convective Heat Transfer

Convective heat transfer occurs when there is a temperature difference between a solid body, (T_s), and its surrounding fluid, T_∞. The convective heat flux, q'' from the solid surface to the surrounding fluid is related to the temperatures T_s and T_∞ through a convection coefficient, h. The main task in analysis of a convective heat transfer problem is to determine the convection coefficient.

It is convenient to formulate the convection coefficient through the non-dimensional Nusselt number, $Nu = \frac{hl}{k_f}$. Here h is the convection coefficient, which is a property of both the fluid and the flow. The quantities l and k_f are respectively an appropriate length scale for the given geometry, and the conduction coefficient of the cooling fluid. The Nusselt number for forced convection in a given geometry is a function of the non-dimensional Reynolds, Re, and Prandtl, Pr, numbers: $Nu = f(Re, Pr)$. The Reynolds number is defined as $Re = \frac{Ul}{\nu}$, where U, l, and ν are respectively a velocity scale of the flow, a length scale of the geometry, and the dynamic viscosity of the cooling fluid. The Prandtl number is defined as $Pr = \frac{\nu}{\alpha}$, where ν is the kinematic viscosity of the cooling fluid, and $\alpha = \frac{k_f}{\rho c_p}$. The quantities k_f, ρ and c_p refer respectively to the heat conduction coefficient, the density and the specific heat at constant pressure, and are properties of the cooling fluid.

The non-dimensional forms of the x-momentum, and energy equa-

tions read

$$u^*\frac{\partial u^*}{\partial x^*}+v^*\frac{\partial u^*}{\partial y^*}=-\frac{dp^*}{dx^*}+\frac{1}{Re}\frac{\partial^2 u^*}{\partial y^{*2}}$$
$$u^*\frac{\partial T^*}{\partial x^*}+v^*\frac{\partial T^*}{\partial y^*}=\frac{1}{RePr}\frac{\partial^2 T^*}{\partial y^{*2}}$$

where

$$x^*\equiv\frac{x}{l},y^*\equiv\frac{y}{l},u^*\equiv\frac{u}{U},v^*\equiv\frac{v}{U},p^*\equiv\frac{p_\infty}{\rho U^2},T^*\equiv\frac{T-T_s}{T_\infty-T_s}$$

Therefore $u^*=u^*(x^*,y^*,Re,dp^*/dx^*)$, and $T^*=T^*(x^*,y^*,Re,Pr)$. The shear stress at the wall surface, τ_s, and the friction coefficient, C_f, are defined as

$$\tau_s=\mu\frac{\partial u}{\partial n}|_{n=0}=\frac{\mu U}{l}\frac{\partial u^*}{\partial n^*}|_{n^*=0}$$
$$C_f\equiv\frac{\tau_s}{\frac{1}{2}\rho U^2}=\frac{2}{Re}\frac{\partial u^*}{\partial n^*}|_{n^*=0}$$

At a solid wall the heat transfer is assumed to occur by pure conduction (no advection). The heat flux is found through the Fourier's law of cooling, $q''=-k_f\frac{\partial T}{\partial n}|_{n=0}$. The convection coefficient, h, is then found through equating the Fourier's law of cooling with the Newton's law, $q''=h(T_s-T_\infty)$. The convection coefficient is thus found as

$$h=\frac{-k_f\partial T/\partial n|_{n=0}}{T_s-T_\infty}=-\frac{k_f(T_\infty-T_s)}{l(Ts-T_\infty)}\frac{\partial T^*}{\partial n^*}|_{n^*=0}=\frac{k_f}{l}\frac{\partial T^*}{\partial n^*}|_{n^*=0}$$

It is thus concluded that the convection coefficient is a function of the flow characteristics and the fluid properties. Rearrangement gives

$$Nu=\frac{hl}{k_f}=\frac{\partial T^*}{\partial n^*}|_{n=0}$$

That is, the Nusselt number is the dimensionless temperature gradient at the wall surface.

The non-dimensional x-momentum and energy equations are very similar, and their wall boundary conditions demand $T^*=u^*=0$. The two equations will have an identical form in the special case of $Pr=1$ and $dp^*/dx^*=0$. In that case

$$\frac{\partial T^*}{\partial n^*}|_{n^*=0}=\frac{\partial u^*}{\partial n^*}|_{n^*=0}$$
$$Nu=\frac{C_fRe}{2}$$

and the friction coefficient, which is more available in the literature, can be used to determine the Nusselt number. The temperature gradient at the wall is thus related to the velocity gradient at the wall. The Prandtl number for air is close to 1 ($Pr_{air} = 0.7$), and the pressure gradient, dp^*/dx^*, along the stator cooling channels is small.

1.3 Objectives and Scope

The aim of this work is to develop a numerical approach to precisely predict the cooling air flow in electric generators, for future use in convective heat transfer analysis. The usual approach is to specify the experimentally measured velocity distribution, or volume flow rate, at the inlet of the computational domain. A limitation of that approach is the difficulty in performing detailed experimental measurements at a high level of accuracy. Electric generators are complex in geometry and are usually packed with different components. This results in a very limited accessibility and leaves a minimal space for positioning the measurement equipment. Another problem is the determination of the turbulence quantities at the inlet, which is even more difficult than the determination of the velocity distribution. Using a fully predictive numerical approach the dependence of the simulations on experimental measurements is removed, while the flow is predicted at a high accuracy. The present work is dedicated solely to the flow of the cooling air, and is thus performed without heat transfer.

The present work includes parametric studies of the influence of the geometry of different components, on the cooling air flow in electric generators. The knowledge gained from the parametric studies is used to modify the design of a real generator, for experimental measurements. The cooling air flow is visualized using a smoke pen, and is measured using 5-hole and total pressure probes. The experimental data is used to validate the numerical results. A simplified half-scale model of the generator is designed and constructed for further validation of the numerical results. The design is determined from both experimental and numerical requirements. It allows geometry and mesh parametrization, it is adapted for mesh quality requirements, and it provides good accessibility for experimental measurements. The knowledge gained in the previous steps of the work is used extensively in the design of the half-scale rig. Experimental measurements, including total pressure and PIV, are performed on the half-scale rig. Two different numerical approaches are used to simulate the cooling air flow. In a fully predictive approach the inlet and outlet boundaries are removed from the computational domain, and the flow is completely

determined by the solution. In another, more common approach, inlet and outlet boundaries are included in the computational domain. The volume flow rate in that case is determined from the experimental measurements and is set through the inlet boundary conditions. The results of the fully predictive numerical approach are found to be closer to the experimental data than those of the approach with inlet and outlet boundary conditions.

Chapter 2

Methodology

THE numerical and experimental methodologies used in the present work are here described.

2.1 Computational Fluid Dynamics

The OpenFOAM-1.5.x CFD toolbox (www.openfoam.org) is used for the numerical simulations in the present work. The steady-state Reynolds Averaged Navier-Stokes equations are solved using the finite volume method. Some of the main methods used in the simulations are here briefly described.

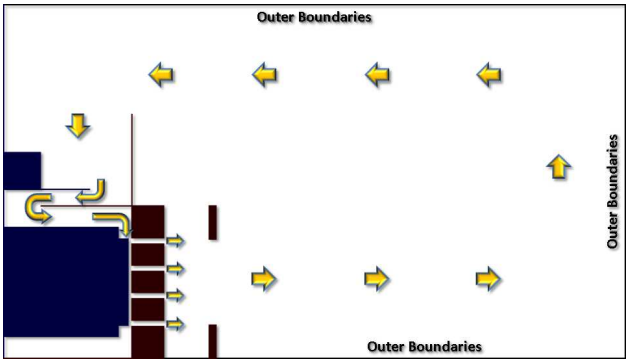

Figure 2.1: Computational domain in the fully predictive approach

Fully Predictive Numerical Approach A part of the space outside the generator is included in the computational domain to allow for re-circulation of the cooling air, see Fig. 2.1. Depending on the boundary conditions used, the cooling air flow may (or may not) freely enter or exit the outer boundaries of the computational domain. No inlet and

outlet boundaries are thus specified in the computational domain. The simulated flow is thus solely driven by the movement of the rotating parts in the computational domain.

Frozen Rotor The numerical studies are performed in steady-state mode, using the Multiple Reference Frame based Frozen-Rotor approach. In this approach the relative position of the rotor and stator meshes is unchanged. The computational domain is instead divided into regions of rotating and stationary reference frames, separated by an axisymmetric interface. An extra source term in the momentum equation includes the effect of the rotation in the rotating region. The frozen-rotor formulation of the momentum and continuity equations is given by

$$\nabla \cdot (\vec{u}_R \otimes \vec{u}_I) + \vec{\Omega} \times \vec{u}_I = -\nabla(p/\rho) + (\nu + \nu_t)\nabla^2 \vec{u}_I \tag{2.1}$$

$$\nabla \cdot \vec{u}_I = 0 \tag{2.2}$$

Variables $\vec{u}_I$ and $\vec{u}_R$ refer to the inertial and relative velocity vectors, respectively, where $\vec{u}_I = \vec{u}_R$ in the stationary region. $\vec{\Omega}$ specifies the rotation vector, which is zero in the stationary region. It is thus the inertial velocity that is solved for, using relative fluxes in the momentum equation divergence term.

The frozen-rotor concept has the disadvantage that the interaction between the rotor and stator is frozen in the tangential direction. However, for the purpose of the present work it is sufficient with a rotor model that provides the correct pressure build-up in the stator. It is shown that the current method is capable of predicting most of the flow details accurately despite this disadvantage.

Turbulence Modeling The turbulence is modeled using the low-Re $k - \varepsilon$ Launder and Sharma turbulence model to correctly handle the low-Re flow in the stator cooling channels. The choice of the Launder and Sharma $k - \varepsilon$ turbulence model is based on a detailed study of the RANS turbulence models implemented in OpenFOAM-1.5.x. The study of the turbulence models is found in Report A, which is summarized in the appendix. The Launder and Sharma $k - \varepsilon$ turbulence model reads

Table 2.1: Launder-Sharma $k-\varepsilon$ turbulence model parameters

ν_t	ε	D	R_T	f_μ
$C_\mu f_\mu \frac{k^2}{\tilde{\varepsilon}}$	$\tilde{\varepsilon}+D$	$2\nu\left(\frac{\partial\sqrt{k}}{\partial x_j}\right)^2$	$\frac{k^2}{\nu\tilde{\varepsilon}}$	$e^{\frac{-3.4}{(1+R_T/50)^2}}$

$$\frac{Dk}{Dt} = \left[\left(\nu + \frac{\nu_t}{\sigma_k}\right)k_{,j}\right]_{,j} + \nu_t\left(u_{i,j}+u_{j,i}\right)u_{i,j} - \varepsilon \tag{2.3}$$

$$\frac{D\tilde{\varepsilon}}{Dt} = \left[\left(\nu + \frac{\nu_t}{\sigma_\varepsilon}\right)\tilde{\varepsilon}_{,j}\right]_{,j} + c_{1\varepsilon}\nu_t\frac{\tilde{\varepsilon}}{k}\left(u_{i,j}+u_{j,i}\right)u_{i,j} - c_{2\varepsilon}(1-0.3e^{-R_T^2})\frac{\tilde{\varepsilon}^2}{k} + 2\nu\nu_t\left(\frac{\partial^2 u_i}{\partial x_j^2}\right)^2 \tag{2.4}$$

Table 2.1 shows the model parameters. The turbulence quantities k and $\tilde{\varepsilon}$ are set to zero at the walls. The computational mesh is required to keep the wall y^+ values at 1.

Numerical Schemes In papers I-III, the divergence term in the momentum equation is discretized using the second-order accurate "Linear Upwind" scheme. In papers IV and V, that term is discretized using the "Limited Linear" scheme, which is a second-order accurate central differencing scheme with a limiter function to remove numerical oscillations. The advection terms in the transport equations of the turbulence quantities are discretized using a first-order upwind numerical scheme.

2.2 Experimental Measurements

The cooling air flow in a real electic generator and a half-scale model is experimentally visualized and measured, using the methods described below.

Flow visualizations The cooling air flow at the inlet of the machines is visualized using smoke pens, see Fig. 2.2. The smoke pens have the advantage of producing intensive smoke despite their small sizes. This makes them practical in flow visualizations where the accessibility is limited.

Figure 2.2: Smoke pen at the inlet of the generator

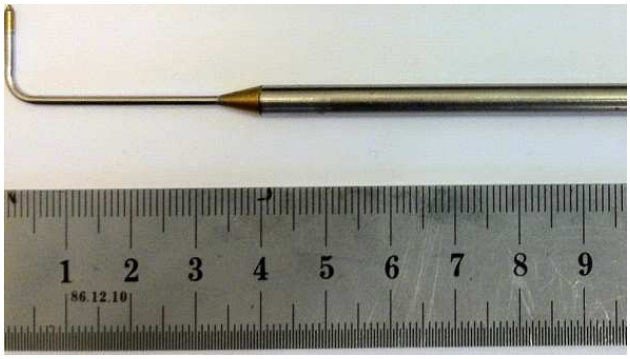

Figure 2.3: 5-hole Probe

5-hole pressure probe measurements The 5-hole pressure probe measurements allow for the separation of the flow components. The 5-hole probe used in this work is manufactured and calibrated by the Aeroprobe Corporation, see Fig. 2.3. The diameter of the probe tip is 1.6 mm with individual distances between the holes of 0.5 mm, and a tip half-cone angle of $30°$. The calibration is performed by the Aeroprobe company, and for 2563 angular positions at a velocity of 20 m/s for pitch and yaw angles varied within $\pm 55°$. The measurement accuracy is better than 1% for the velocity magnitude and $0.5°$ for the flow angles.

Total pressure measurements The total pressure measurements at the machine outlet are performed using total pressure rakes, see Fig. 2.4. At the inlet the total pressure is measured with a single tube L-shaped total pressure probe (similar to the 5-hole probe). Together with a local static pressure measurement, the velocity magnitude along

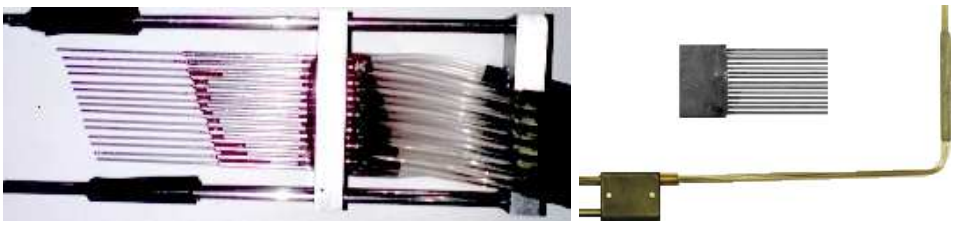

(a) Full-scale generator (b) Half-scale model

Figure 2.4: Total pressure rakes

the probe direction is found as:

$$|U| = \sqrt{2(p_{tot} - p_{stat})/\rho} \tag{2.5}$$

The total pressure probe tubes are calibrated for pitch and yaw angles within $\pm 10°$. To maintain the highest possible accuracy in a low-pressure range, the pressure transducers are regularly controlled for an offset and nulled before each set of measurements. The resulting precision of the transducer offset is better than 0.2 Pa.

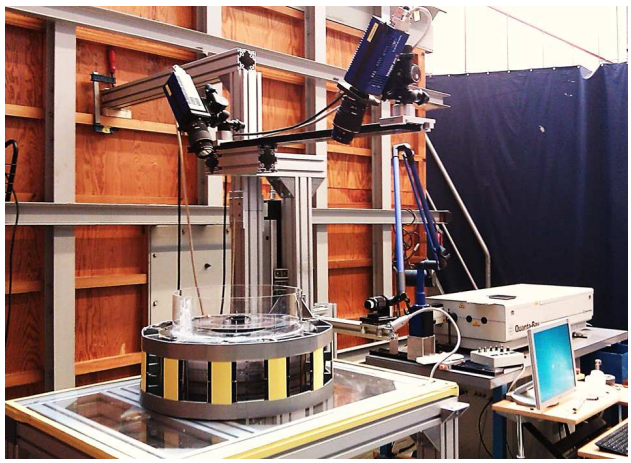

(a) Experimental rig and camera system

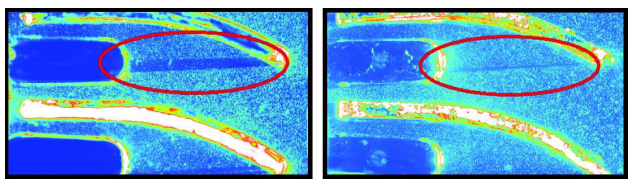

(b) PIV-images of the flow in the stator channels

Figure 2.5: PIV measurements

PIV measurements Velocity distributions can be found using Particle Image Velocimetry (PIV) measurements, see Fig. 2.5. A thin laser sheet is positioned in the flow. The flow contains small particles which are illuminated by the laser sheet once passing through the measurement plane. The cameras register the position of the particles in two consecutive frames. A comparison of the particle locations in the two frames determines their displacements. Knowing the time difference between the frames, the particle velocities, and thus the flow velocity distribution in the measurement plane is determined. The stereo camera angle in the experiments is set to 60°, the camera distance is 600 mm away from the horizontal measurement plane, and the laser sheet thickness is 2-4 mm. The cameras and laser head are mounted on a single frame, enabling simultaneous traversing of the system without re-adjustment. The system calibration is performed using a standard calibration plate, Type11. The flow is sliced with a 1 mm step in the axial direction. The flow is seeded with smoke droplets of average size 1 μm. To avoid possible effects of rig displacements in the PIV measurements, the image capturing is synchronized to the rotor position. Averaging is done over 150 data samples to examine the velocity distribution in the inlet region. In the PIV processing, a 64x64 - 32x32 pixel window with 50% overlapping is used in multi-pass mode. The particle concentration is higher than optimal, to suppress the intensive radiation scattered by dust particles on the surfaces and to improve the velocity field quality. The inner parts of the rig are coated by reflective and absorbing material to significantly reduce scattered radiation from the irradiated laser sheet light. The arrangement allows registering of particle patterns of 1-2 mm above the rotor surface. The errors in the PIV velocity field is estimated to 0.34 m/s due to the 0.2 pixel error in the sub-pixel interpolation.

Figure 2.5(b) shows PIV images of the flow in the transparent stator channels. A shadow region is marked in the images. The baffles are modified to reduce the shadow, leading to an 85% reduction in the shadow area.

Chapter 3

Summary of Papers

THIS chapter gives a short summary of the main contents and results reported in the papers on which this thesis is based.

3.1 Paper I

Motivation and Background Paper I is dedicated to the development of a preliminary understanding of the cooling air flow in electric generators. The aim is to investigate the effect of geometrical details of the rotor and stator on the flow characteristics inside the machine.

Main content and Results The numerical simulations in paper I are performed using the fully predictive approach, where the surrounding boundaries of the computational domain are assigned a slip-wall boundary condition. The flow is thus allowed to recirculate in the computational domain. Figure 3.1 shows an example of the generator ge-

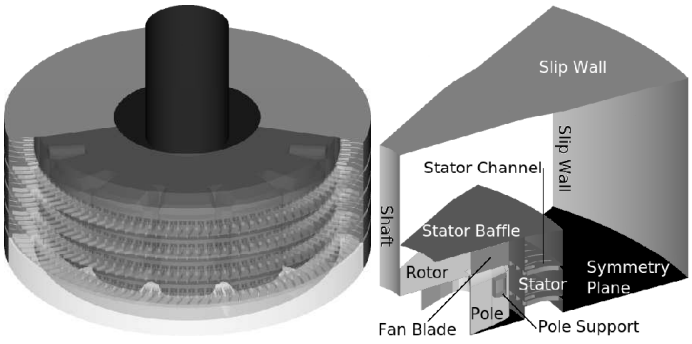

(a) Generator CAD (b) Computational domain

Figure 3.1: The generator geometry in paper I

ometry that is used in paper I. The cooling air flows axially into the generator from both sides of the stator, and the flow is assumed to be evenly distributed between the two inlets. The computational domain is therefore reduced using a symmetry plane in the middle of the generator. The computational domain is also tangentially reduced to a 1:12 sector, using cyclic boundary conditions at the sides. The simplest rotor geometry has radial poles, and the poles are modified in seven steps. The final rotor geometry is a close representation of a real generator, located at Uppsala University, Sweden. For each rotor geometry, three different simulations are performed: a simulation with a base stator, a simulation with added horizontal baffles at the stator inlet, and a simulation with the horizontal baffles and with radial fan blades on the rotor poles.

Although not experimentally validated, the numerical results from paper I yield useful knowledge that is used in the further development of this work. The addition of the stator baffles increases the volume flow rate in the machine, while it reduces the required rotor axial power that drives the flow. The use of the rotor fan blades combined with the stator baffles drastically increases both the volume flow rate and the required rotor axial power. The flow in the stator cooling channels is shown to be associated with large separation and recirculation regions. The recirculation regions in the stator channels decrease in size with an increasing volume flow. The recirculation regions are thus smallest in the cases with fan blades and stator baffles.

Comments The numerical results in paper I are not experimentally validated, and are thus only used for relative comparisons of the effect of the geometrical modifications.

3.2 Paper II

Motivation and Background From the studies in paper I, it is concluded that the use of stator baffles can increase the volume flow rate through the machine considerably. A combination of stator baffles and rotor fan blades proves to increase the volume flow rate through the machine even more. These learning outcomes are used to modify the generator rig at Uppsala University for experimental measurements of the cooling air flow, and a first validation of the numerical methodology is performed.

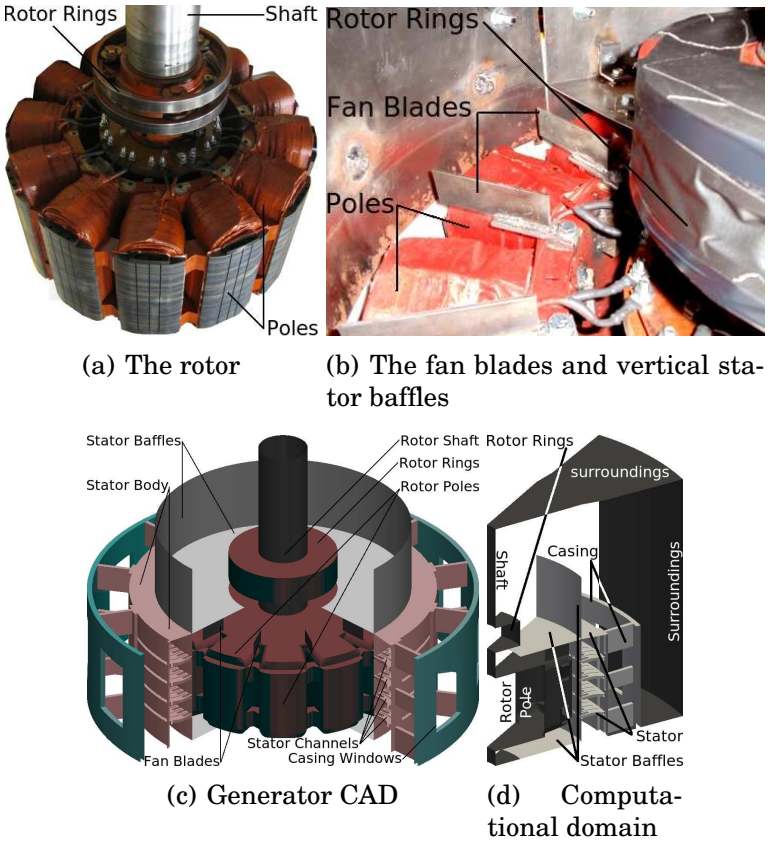

(a) The rotor

(b) The fan blades and vertical stator baffles

(c) Generator CAD

(d) Computational domain

Figure 3.2: The generator geometry in paper II

Main content and Results Figure 3.2 shows the generator studied in paper II. The inlet at the bottom of the machine is clogged, and the cooling air flows into the generator from above the machine. This is done to avoid the possible asymmetric flow distribution that could occur with two inlets. The computational domain thus includes the entire generator height. The generator is provided with stator baffles and rotor fan blades to increase the volume flow rate through the machine. Experimental flow visualizations and measurements are performed, to validate a new numerical simulation. The flow visualizations are performed with a smoke pen at the machine inlet. The flow measurements are performed using a 5-hole pressure probe at the inlet, and a total pressure rake at the outlet. The numerical simulation is performed using the fully predictive approach. The geometry used in the experiments is partly blocked by the cables and rig mountings. The extra blockage at the outlet is not included in the numerical geometry. Although geometrical differences between the numerical and experimental cases are present, velocity distributions at the machine inlet and at the stator channel outlets demonstrate very similar trends.

However, a quantitative comparison shows that the volume flow rate is over-predicted by the numerical simulation.

Comments The numerically predicted volume flow rate in the paper is by mistake concluded to be $0.164m^3/s$, where the correct value should be $0.109m^3/s$. The over-estimation of the volume flow rate by the numerical simulation is thus reduced to 28%, compared to the experimentally *estimated* value. The experimental data shows considerable tangential asymmetry in the flow inside the generator. The asymmetry in the measured flow is caused by the asymmetry in the rig geometry, which is not included in the computational domain.

3.3 Paper III

Motivation and Background The numerical simulation in paper II is concluded to significantly over-estimate the experimentally estimated volume flow rate through the machine. However, a comparison of the velocity distributions at the inlet and outlet shows that the numerical predictions demonstrate similar flow patterns to those experimentally measured. The focus in paper III is to investigate the effect of different rotor speeds on the predicted flow pattern, and to find a correlation between the flow characteristics and the rotational speed of the rotor.

Main content and Results Four numerical simulations are performed with the fully predictive approach. The computational domain is identical as the one used in paper II, and the simulations differ only in the rotor rotational speed. The normalized numerical results are compared to each other and to the experimental data from paper II. The volume flow rate is concluded to increase linearly with the rotor rotational speed, while the required rotor axial power to drive the flow follows a cubic relation with the rotational speed of the rotor. The recirculation areas in the stator cooling channels are reduced with an increased rotational speed of the rotor.

Comments The normalized velocity and static pressure distributions inside the machine are similar at all speeds. The largest inward axial velocities are observed between the poles and close to the trailing edge, where the pressure is lowest. At the leading edge there are only upward axial velocities as the flow is deflected upwards when meeting

the pole from below the fan blades. Just above the pole surface the axial velocity is zero. The axial velocity tends to be more inwards near the stator inner wall.

3.4 Paper IV

Motivation and Background A well-defined inlet geometry favors the quality of the inlet measurement, and makes it easy to set up numerical simulations with inlet boundary conditions. The generator rig at Uppsala University is therefore modified to better define the inlet boundary. The rotor fan blades are also modified. Paper IV presents new flow measurements and simulations on the generator rig at Uppsala University after geometrical improvements.

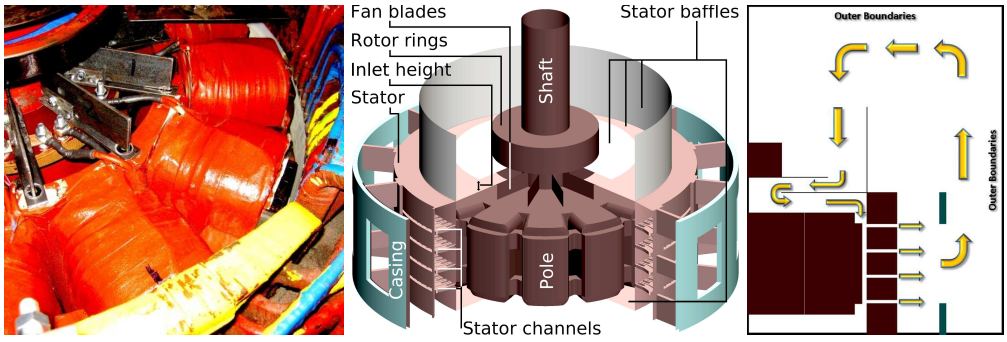

(a) Rotor fan blades (b) Generator CAD (c) Computational domain

Figure 3.3: The generator geometry in paper 4

Main content and Results Figure 3.3 shows the generator geometry used in paper IV. A new horizontal baffle is added to the stator to better define the inlet, and the rotor fan blades are moved to the shaft. A new set of experimental measurements are performed on the modified rig. The flow at the inlet is measured by two different 5-hole probe measurements, and a total pressure probe measurement. The flow at the stator channel outlets is measured by the same total pressure probe rake as in papers II and III. The experimental data is used to assess the numerical results from two different numerical approaches: the fully predictive approach, and with inlet and outlet boundary conditions. The numerical simulations using the fully predictive approach show that the use of a constant total pressure outer boundary condition yields a better flow prediction than slip wall boundary conditions. The numerical simulations using inlet and outlet boundary conditions

are designed to investigate the sensitivity of the results to the level of detail in the inlet boundary conditions. The level of details in the inlet boundary conditions proves to play an important role in predicting the flow pattern in the machine.

Comments Although the volume flow rate is under-estimated by the fully predictive numerical approach, it yields very similar flow behavior to that experimentally measured. The experimental data shows a scattering at the stator outlet, caused by geometric imperfections. However, the numerical velocity distributions at the stator outlets are close to the mean of the experimental data in each channel. A more accurate determination of the experimental volume flow rate would be possible through measurements at more tangential positions at the inlet. This is however not done as a result of accessibility limitations in the rig.

3.5 Paper V

Motivation and Background The measurements in the Uppsala generator, presented in papers II-IV, suffer from some restrictions. Being a real electric generator, the access for flow measurements is highly restricted, and some of the air flow paths are blocked with electric equipment. A half-scale model of the Uppsala generator is therefore designed and built for detailed measurements of the cooling air flow under well-defined conditions.

Main content and Results A simplified half-scale model of the Uppsala generator is designed and built exclusively for measurements of the cooling air flow. Figure 3.4 shows the rig and some experimental and numerical details. The scale model is provided with optical access to allow for flow measurements with Particle Image Velocimetry, PIV, and with built-in pressure probes to allow for static pressure measurements inside the machine. Two stator geometries are manufactured to investigate the influence of the cooling channel curvature on the flow. The Reynolds similarity between the half-scale model and the full-scale generator is preserved by quadrupling the rotational speed of the rotor in the half-scale model.

The flow details at the inlet and inside the machine is measured using PIV, and the outlet flow distribution is measured using a total pressure rake. The experimental data is used for validation of numerical results performed with two approaches: the fully predictive approach

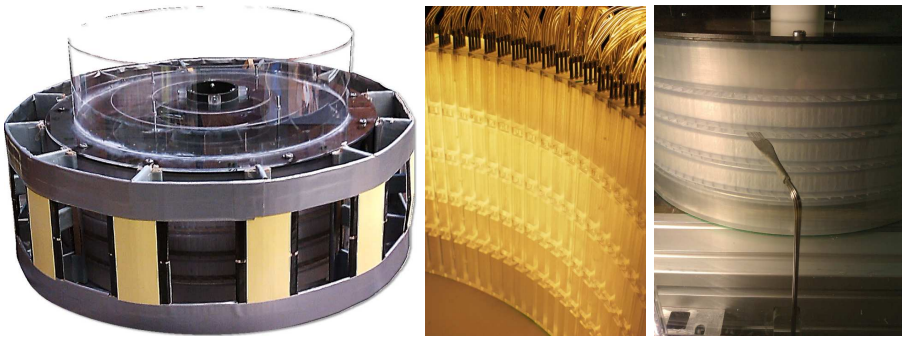

(a) The rig

(b) The built-in pressure probes

(c) The rake at the channel outlets

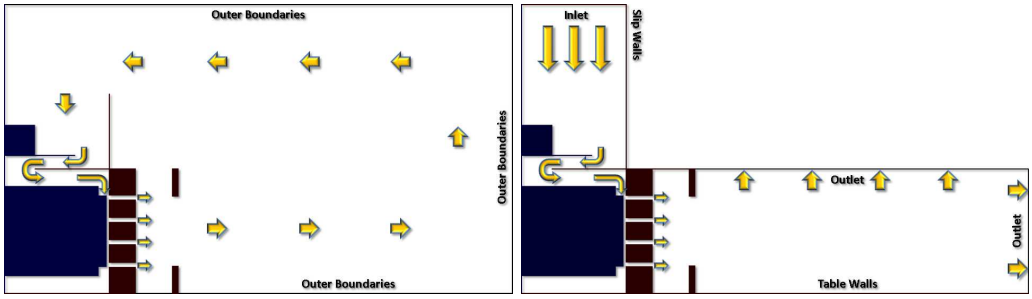

(d) FP Computational domain

(e) BC Computational domain

Figure 3.4: The half-scale generator model in paper V

(FP), and with inlet and outlet boundary conditions (BC), as shown in Fig. 3.4. The volume flow rates at the inlet of the numerical simulations with inlet and outlet boundary conditions are estimated from the experimental measurements, as in the Uppsala generator. It is found that the fully predictive approach yields the most accurate results. The flow rate is within 2% of that experimentally estimated, and the flow details agree to a large extent with the experimental data.

Comments The volume flow rates in the measurements are estimated assuming a constant velocity distribution in the unmeasured part of the PIV measurement cross-section. The error introduced by the assumption is believed to be comparable to the error in the predicted volume flow rate. The very good agreement of the numerical results using the fully predictive approach suggest that the approach is capable of predicting the flow inside generators at a high precision.

Chapter 4

Conclusions and Future Work

A fully predictive numerical approach is assessed for the simulation of cooling air flow in electric generators. An accurate flow prediction is a necessary first step towards an accurate convective heat transfer analysis. The numerical approach is assessed using experimental measurements on a real generator rig, and on a half-scale specialized laboratory model rig. The numerical approach is applied to cases with different geometrical modifications and with different boundary conditions on the outer boundaries of the computational domain. With a sufficiently high mesh resolution and appropriate outer boundary conditions, the approach proves to be able to predict the flow details at a high level of accuracy. The volume flow rate predicted by the numerical simulations agrees well with the experimental data that is determined under well-defined conditions. The accurate prediction of the flow field indicates that the flow losses and wall shear stresses are simulated at a high accuracy. An accurate prediction of the wall shear stresses is highly related to an accurate prediction of the convective heat transfer.

The studies in the present work reveal considerable flow losses which can be reduced by a better design. A better design and positioning of the rotor fan blades, a better design of the stator cooling channels, a smaller rotor-stator air-gap, etc. can help reducing the losses.

The simulations presented in this work are performed in steady-state, using the frozen-rotor concept. Although capturing many details of the time-averaged flow, many flow structures are instantaneous and remain uncaptured using this method. Time-resolved flow simulations are thus necessary to capture all the flow details. Accurate convective heat transfer simulations may only be performed when the flow field is predicted at a high accuracy.

Appendix A

Additional Relevant Publications

A number of relevant publications which are not a part of this thesis are here summarized, for further reference.

A.1 Report A

Moradnia, P., 2010. "CFD of air flow in hydro power generators". Thesis for licentiate of engineering, no. 2010:11, Chalmers University of Technology, Gothenburg, Sweden

http://publications.lib.chalmers.se/publication/129342

Division of work Moradnia produced all the numerical results and wrote the report. Nilsson supervised the planning, analysis and writing. The final version was proofread by both Moradnia and Nilsson.

Motivation and Background Selection of an appropriate turbulence model is of high importance when performing numerical simulations of turbulent fluid flow. The choice of the Launder-Sharma $k-\varepsilon$ turbulence model for the numerical simulations in the present work is based on a thorough study of the turbulence models implemented in OpenFOAM-1.5.x.

Main content and Results A detailed study of the RANS turbulence models in OpenFOAM-1.5.x is presented in report A. The investigated turbulence models in OpenFOAM include:

- kEpsilon: Standard $k-\varepsilon$ with wall functions

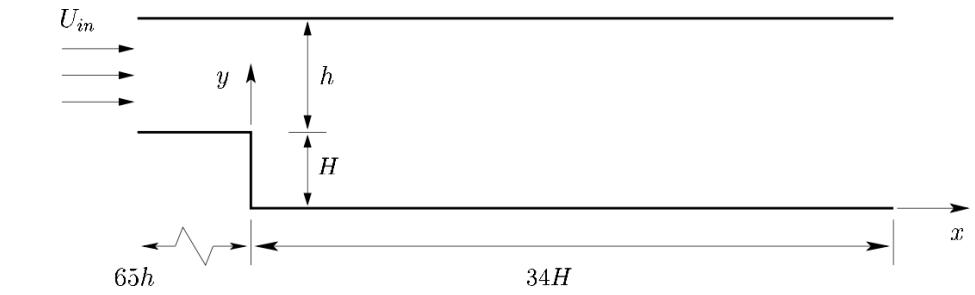

(a) geometry

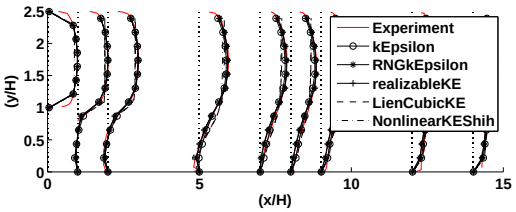

(b) High-Re $k-\varepsilon$ models

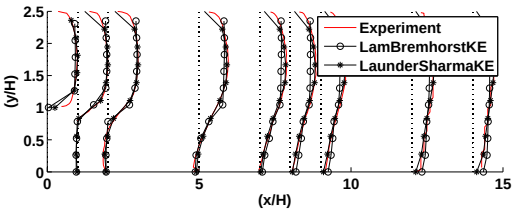

(c) Low-Re $k-\varepsilon$ models

Figure A.1: The backward facing step case

- RNGKEpsilon: $k-\varepsilon$ using Re-normalization Groups method, with wall functions
- realizableKE: Realizable $k-\varepsilon$ with wall functions
- kOmegaSST: $k-\omega$ SST
- NonlinearKEShih: Non-linear Shih $k-\varepsilon$ with wall functions
- LienCubicKE: Cubic $k-\varepsilon$ by Lien, with wall functions
- QZeta: Low-Re $Q-\zeta$
- LaunderSharmaKE: Low-Re Launder-Sharma $k-\varepsilon$
- LamBremhorstKE: Low-Re Lam-Bremhorst $k-\varepsilon$
- LienLeschzinerLowRe: Low-Re Lien-Leschziner $k-\varepsilon$
- LienCubicKELowRe: Low-Re Cubic $k-\varepsilon$ by Lien
- LRR: RSTM model by Launder, Reece and Rodi
- LaunderGibsonRSTM: RSTM model by Launder and Gibson
- SpalartAllmaras: 1-equation mixing length model by Spalart and Allmaras

The implementations in OpenFOAM are described and compared to the corresponding descriptions in literature. In some cases, certain differences between the original model and the OpenFOAM implementation are found. The turbulence models are tested for the flow over a backward facing step, see Fig. A.1(a). The numerical results are validated with available experimental data, see Fig. A.1(b,c).

The report also includes a validation of the numerical simulations of a laminar Couette flow with the corresponding theoretical solution, as well as a description of the numerical schemes used.

Comments The studies in report A provide an important foundation for the selection of an appropriate turbulence model for the numerical simulations in this thesis. The low-Re flow in the stator cooling channels demands a low-Re turbulence model. The LaunderSharmaKE model proves to yield similar results as the experimental data. It also proves to be less sensitive to the mesh resolution than the other low-Re models. The numerical simulations of the cooling air flow in electric generators in this thesis are thus performed using the LaunderSharmaKE model.

A.2 Report B

Moradnia, P., Nilsson, H., Page, M., Beaudoin, M., Torriano, F., Morissette, J., and Toussiant, K., 2012. "Transient and steady-state air flow simulations in generators using OpenFOAM", ISSN 1652-8549, Internal report nr 2012:12 Chalmers University of Technology, Gothenburg, Sweden

http://publications.lib.chalmers.se/publication/156234

Division of work Moradnia produced all numerical results with OpenFOAM, and wrote the report. Toussaint produced all numerical results with CFX. Page supervised the planning and analysis. Beaudoin provided technical support and consultation. Torriano and Morissette provided consultation. Nilsson supervised the planning, analysis and writing. The final paper was proofread by Moradnia and Nilsson.

Motivation and Background There are many parameters that play an important role in reaching numerical stability and accurate numerical results. The numerical simulations in papers IV and V are per-

formed using the knowledge gained from the studies presented in report B.

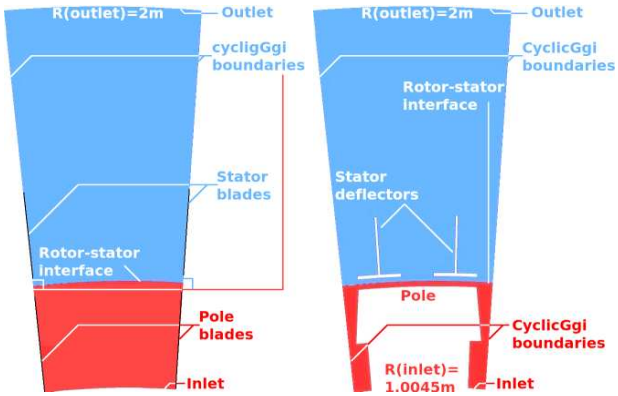

(a) "Generator" with radial rotor and stator blades

(b) Generator with more realistic rotor and stator geometries

Figure A.2: Two geometries used in the numerical simulations

Main content and Results The air flow in two 2D geometries, representing highly simplified generators, is simulated with OpenFOAM-1.6-ext (see Fig. A.2). The results are compared to those obtained with CFX. Different simulation strategies, numerical methods, turbulence models, linear solvers, preconditioners, mesh resolutions, rotor-stator interface type, location and boundary conditions are investigated. An analysis of the effect on the flow details is provided. The numerical convergence, the required computational effort, the obtained flow field, the required axial rotor torque, and the windage losses are studied in each case. It is shown that a good combination of the parameters saves much of the computational effort, and improves the precision of the numerically predicted flow.

The frozen-rotor results are shown to depend on both the relative position of the rotor pole and stator deflectors, as well as the radial position of the rotor-stator interface (RSI). Figure A.3 shows the radial and tangential velocity distributions across the RSI in frozen-rotor simulations with different RSI types. The mesh distribution across the interface, and the boundary conditions used at the interface do not affect the results considerably. Both radial and tangential velocity distributions are found to be largely affected by the interface radial position. This is a result of an intrinsic property of the frozen-rotor concept when transferring wakes across the RSI. The problem vanishes in sliding grid simulations, as the transient flow in each time step is simulated

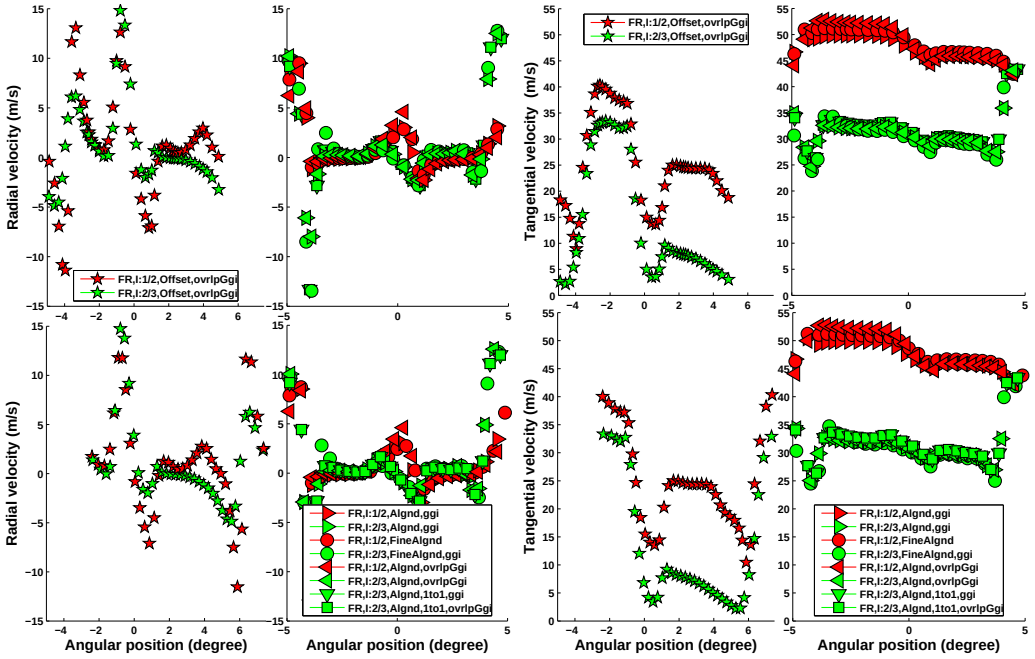

(a) Radial velocities (b) Tangential velocities

Figure A.3: Frozen-rotor results with different RSI types, RSI radial positions, and the relative position of the rotor pole and stator deflectors

with an updated coupling between the rotor and stator regions.

Comments The small size of the stator channels relative to the rotor poles, and the large rotor-stator air gap in comparison to the stator channels in papers I-V reduces the effect of the rotor-stator relative position on the simulation results. The numerical results in report B are not experimentally verified, and are thus only used for relative comparisons between the numerical results.

A.3 Report C

Hartono, E. A., 2011. "Experimental Study of Air Flow in a Hydro Power Generator Model - Design, Construction, and Measurements", Master thesis project report, no. 2011:51, Chalmers University of Technology, Gothenburg, Sweden

http://publications.lib.chalmers.se/publication/147717

Division of work Hartono built the rig, produced the experimental data, and wrote the report. Moradnia provided the geometry, and supervised the design, manufacturing and writing. Chernoray supervised the design, manufacturing, experiments, analysis, and writing. Nilsson supervised the planning, design, manufacturing, analysis, and writing. The final paper was proofread by Hartono, Moradnia, Chernoray, and Nilsson.

Motivation and Background As pointed out in papers II-IV, the experimental data from the full-scale Uppsala generator suffer from restrictions. Detailed flow measurements are impossible to perform as the accessibility in the rig is very limited. The geometry is not prescribed to a high level of accuracy, and it is difficult or impossible to do geometrical modifications. Therefore a half-scale model of the generator is designed and manufactured exclusively for measurements of the cooling air flow.

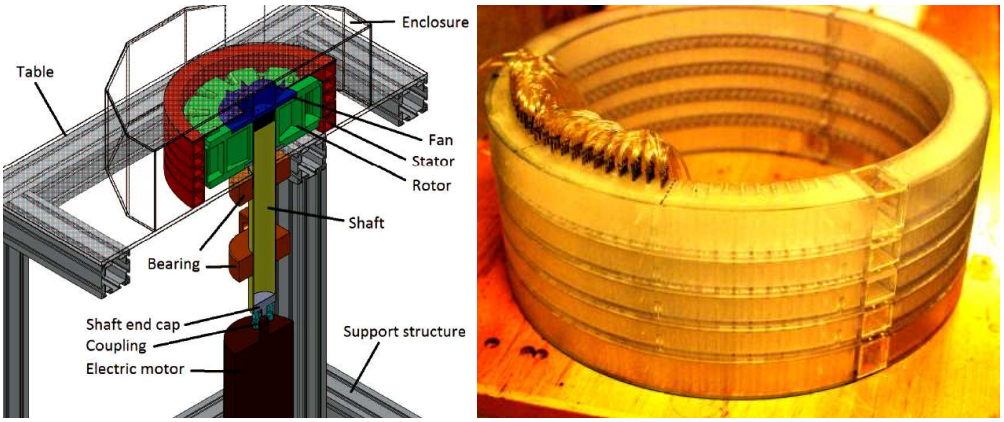

(a) The rig

(b) The stator with pressure measurement tubes and access for PIV

Figure A.4: The half-scale generator model

Main content and Results The rig is designed using the learning outcomes of papers I-IV. It is parametrized for a more efficient and accurate generation of the computational domain and mesh. The rig is provided with optical access for flow measurements with Particle Image Velocimetry, PIV, and with built-in pressure probes for pressure measurements inside the machine, see Fig. A.4(b). The report includes experimentally measured static and total pressure data, as well as a discussion about the volume flow rate variations with fan blade length.

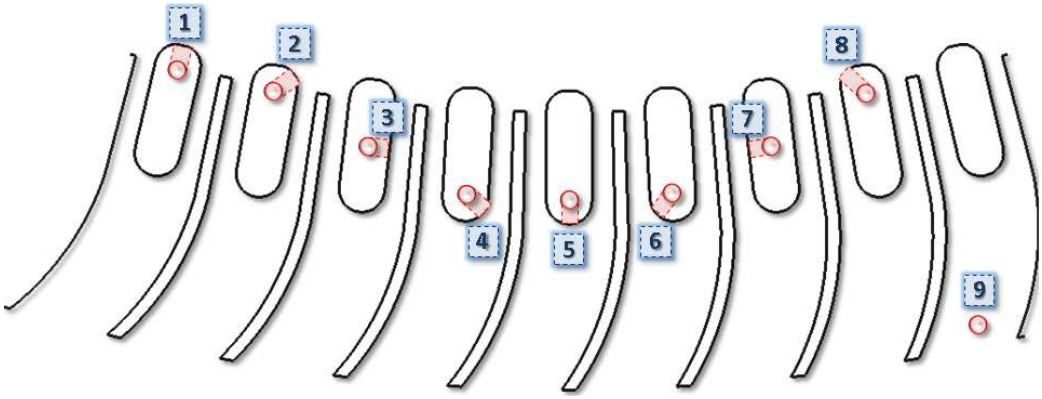

(a) The pressure probes

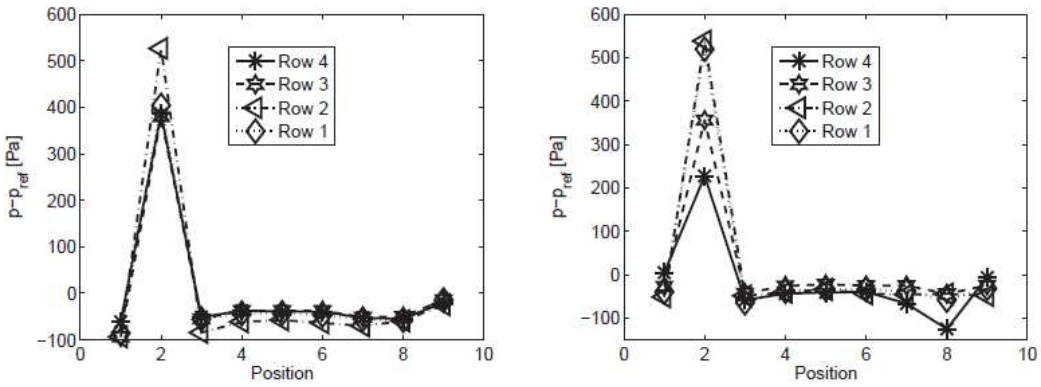

(b) Static pressure in the stator with bent (left) and radial (right) channels

Figure A.5: The pressure probes and measured pressure data in the stator channels

The built-in pressure probes in the half-scale model are designed to give detailed pressure data in the stator channels, as well as inside and outside the stator. Figure A.5(a) shows the pressure probes inside the stator channels in the half-scale model. The static pressure distribution in the stator channels is shown in Fig. A.5(b). The highest static pressure is observed by probe number 2 in both stators, as that probe is located close to the stagnation point.

The total pressure distribution at the stator channel outlets are shown in Fig. A.6. Figure A.6(a) shows the total pressure relative to the reference pressure at the channel outlets. Figure A.6(b,c) shows the total pressure coefficient, $C_{pTot} = \frac{(p_{tot} - \overline{p_{tot,ch}})}{(p_{tot,ch,max} - \overline{p_{tot,ch}})}$, distributions at the channel outlets (for comparison to Paper V). Despite some differences in geometries, the C_{pTot} distributions demonstrate a very similar behavior to those presented in paper V.

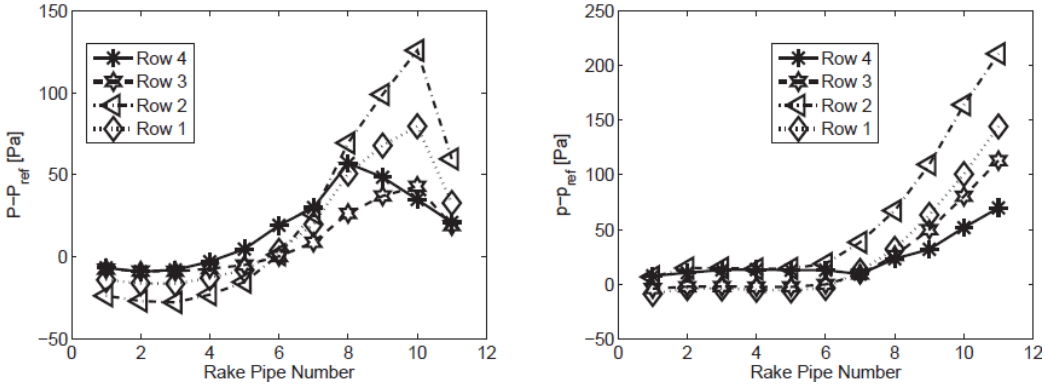

(a) $p_{tot} - p_{ref}$, Stator with bent (left) and the radial (right) channels

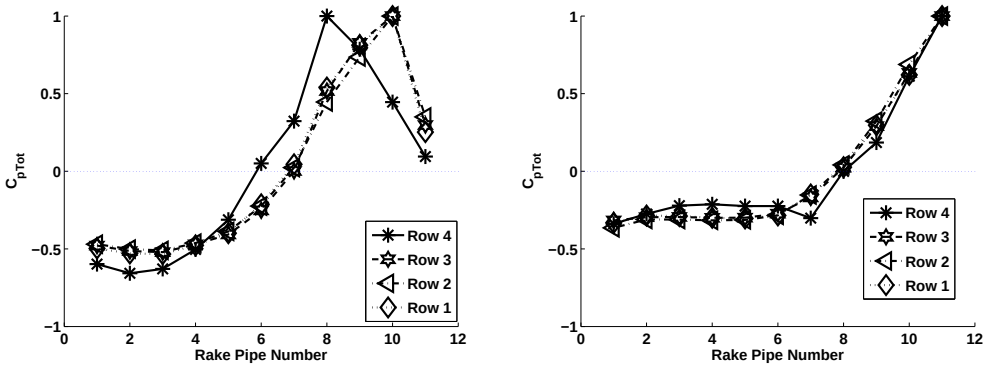

(b) C_{pTot}, stator with bent channels

(c) C_{pTot}, stator with radial channels

Figure A.6: Total pressure at the stator outlets

Comments The experimental measurements in report C are performed with a transparent enclosure around the model, see Fig. A.4(a). The enclosure is designed to represent the outer boundaries of the computational domain in the numerical simulations, yielding a recirculating flow.

A.4 Paper D

Hartono, E. A., Golubev, M., Moradnia, P., Chernoray, V., and Nilsson, H., 2012. "PIV Measurement of Air Flow in a Hydro Power Generator Model", Proceedings of the 16th Int Symp on Applications of Laser Techniques to Fluid Mechanics, Portugal

http://publications.lib.chalmers.se/publication/164017

Division of work Hartono produced all the experimental data and wrote the paper. Golubev was involved in the experiments, performed the analysis, and supervised the writing. Moradnia supervised the writing. Chernoray and Nilsson supervised the planning, experiments, analysis, and writing. The final paper was proofread by all authors.

Motivation and Background The use of the enclosure results in the creation of a large swirl component of the flow outside the generator, which affects the accuracy and usability of the experimental measurements. The swirling flow is also present in the numerically predicted flow field and prevents the numerical convergence, despite a large number of iterations. Also, the set-up and quality of PIV measurements on the half-scale generator rig is to be examined and improved. Paper D reports modifications and successful PIV measurements in the rig.

Main content and Results Detailed PIV measurements are performed in the half-scale generator rig. The half-scale model is surrounded by a transparent enclosure as in report C. Paper D includes PIV measurements at the inlet, inside the stator cooling channels, and outside the stator. A total of 15 measurement planes are created to capture an overall picture of the flow, interpolated to give an overview of the flow field around the stator body. The flow outside the stator proves to be highly swirling due to the presence of the enclosure. Phase-averaged measurements show that the flow structures inside the channels are independent of the rotor pole position. A large flow separation is captured at the inlet.

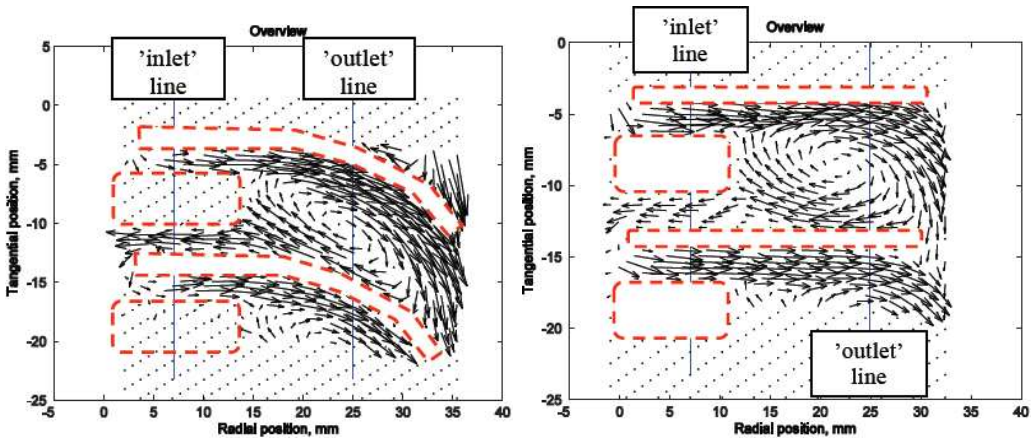

Figure A.7: Velocity vectors from the PIV measurements in the half-scale stators with bent (left) and radial (right) channels

Figure A.7 shows the velocity vectors in the stator cooling channels obtained from the PIV measurements. The flow enters the channels from the upstream side of the stator coils. A large recirculation area is observed downstream of the coils, which extends to the channel outlets. A part of the flow exits the stator channels and re-enters the air gap from the low pressure region downstream of the coils.

Comments A significant part of the work in paper D is spent on improving the PIV measurement quality. The flow patterns inside the stator channels agree with that predicted by previous numerical simulations. A number of numerical simulations are performed with the fully predictive approach on the half-scale model with the enclosure. The presence of the enclosure leads to a large swirl outside the stator which makes the numerical convergence difficult and impairs the simulation accuracy. The simulation results are therefore not published. Instead, the rig is re-designed, and in the studies presented in paper V, the transparent enclosure is removed. The computational domain are replaced by permeable walls with a constant total pressure boundary condition. This gives a much faster numerical convergence, and a much better agreement between the experimental and numerical results. Despite the geometric differences, the flow pattern in the stator channels is identical to those presented in papers I-III, and hence papers IV and V.